

X-GGM: Graph Generative Modeling for Out-of-Distribution Generalization in Visual Question Answering

Jingjing Jiang, Ziyi Liu, Yifan Liu, Zhixiong Nan, Nanning Zheng*

Institute of Artificial Intelligence and Robotics, Xi'an Jiaotong University, Shannxi, China
jingjingjiang2017@gmail.com, {liuziyi, lyf666}@stu.xjtu.edu.cn, {nzx2018, nnzheng}@mail.xjtu.edu.cn

ABSTRACT

Encouraging progress has been made towards Visual Question Answering (VQA) in recent years, but it is still challenging to enable VQA models to adaptively generalize to out-of-distribution (OOD) samples. Intuitively, recompositions of existing visual concepts (*i.e.*, attributes and objects) can generate unseen compositions in the training set, which will promote VQA models to generalize to OOD samples. In this paper, we formulate OOD generalization in VQA as a compositional generalization problem and propose a graph generative modeling-based training scheme (X-GGM) to implicitly model the problem. X-GGM leverages graph generative modeling to iteratively generate a relation matrix and node representations for the predefined graph that utilizes attribute-object pairs as nodes. Furthermore, to alleviate the unstable training issue in graph generative modeling, we propose a gradient distribution consistency loss to constrain the data distribution with adversarial perturbations and the generated distribution. The baseline VQA model (LXMERT) trained with the X-GGM scheme achieves state-of-the-art OOD performance on two standard VQA OOD benchmarks, *i.e.*, VQA-CP v2 and GQA-OOD. Extensive ablation studies demonstrate the effectiveness of X-GGM components. Code is available at <https://github.com/jingjing12110/x-ggm>.

KEYWORDS

graph generative modeling, OOD generalization, VQA

1 INTRODUCTION

Visual Question Answering (VQA) [4], answering questions conditioned on understanding the given image and question, is a task toward general AI [62]. Although considerable progress has been made in VQA, most methods usually process similar data distributions between training and test sets. However, a good VQA model should be robust against answer distribution shift [35] and perform well on out-of-distribution (OOD) testing [61], *i.e.*, evaluating the ability of the model to generalize beyond dataset-specific language biases [1, 2, 20, 75]. This paper focuses on OOD generalization in VQA, aiming to improve the OOD generalization ability of baseline VQA models while preserving their in-domain (ID) performance.

OOD generalization in VQA is challenging. To generalize to out-of-distribution samples adaptively, the VQA model should own two capabilities: (1) overcoming negative language biases and (2) producing out-of-distribution answers by learning rules entailed in in-domain data. The prevailing OOD generalization methods [10, 11, 18, 66] focus on enhancing the first capability, which achieves OOD generalization by explicitly mitigating the language biases. While the second capability, which directly endues VQA models

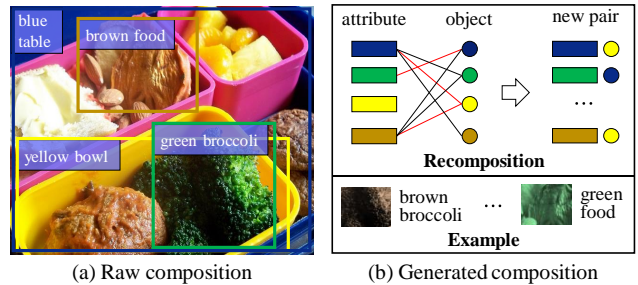


Figure 1: Compositional generalization implied in graph generative modeling. New compositions (*e.g.*, brown broccoli) of attributes and objects can be generated by raw compositions (*i.e.*, green broccoli and brown food).

the potentiality to generalize to out-of-distribution (*i.e.*, unseen or rare) samples, has not been well explored.

Benefiting from good compositional generalization capabilities, humans can easily achieve OOD generalization [42]. Motivated by this, we formulate OOD generalization in VQA as a compositional generalization problem and leverage in-domain data to generate new/raw compositions of existing visual concepts (*i.e.*, attributes and objects) to make VQA models produce out-of-distribution answers. As shown in Figure 1, given any two attribute-object pairs, such as green broccoli and brown food in Figure 1 (a), new compositions (*e.g.*, brown broccoli in Figure 1 (b)) can be generated by graph generative modeling. The abundant recompositions probably contain unseen or rare samples in the training set, promoting the VQA models to generalize to out-of-distribution samples. To represent relationships and generate new compositions of existing visual concepts, Graph Generative Model [65] is the natural preference, which has been proven to have the potential to improve the generalization ability of models [12, 77].

In this paper, we propose X-GGM, a graph generative modeling-based training scheme, to improve the OOD generalization performance of existing VQA models while preserving their representation ability. As shown in Figure 2, X-GGM consists of two key modules, *i.e.*, graph relation generative modeling (R-GGM) and graph representation generative modeling (N-GGM). R-GGM aims to update relationships between nodes to indirectly improve the OOD generalization ability. It first introduces adversarial perturbations (*i.e.*, Gaussian noise) to the cross-modality representation (x) to initialize the relation matrix. After that, it utilizes Graph Encoder to aggregate information of different nodes and to update the relation matrix in an iterative manner. N-GGM targets perturbing node representations to directly enhance the OOD generalization ability. For N-GGM, adversarial perturbations are first injected into the cross-modality representation to initialize node

*Corresponding author.

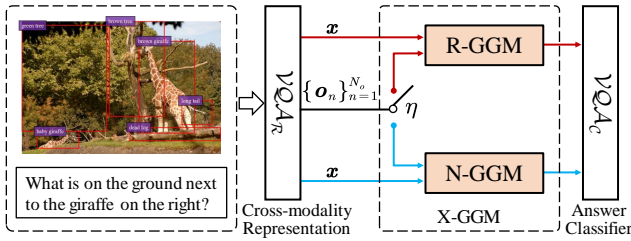


Figure 2: An overview of training a baseline VQA model using the X-GGM scheme. R-GGM and N-GGM are the two key modules of X-GGM. \mathcal{VQA}_R and \mathcal{VQA}_C indicate the Cross-modality Representation and Answer Classifier of a baseline VQA model, respectively.

representations. Subsequently, Graph Encoder is applied to encode node representations and to update representations iteratively.

In addition, X-GGM injects adversarial noises into the cross-modality representation to describe the original data distribution of relation matrices or node representations, leading to an inaccurate prior distribution in graph generative modeling. The inaccurate distribution affects the stability of graph adversarial learning. To alleviate the unstable training issue, we propose a gradient distribution consistency loss. The proposed loss can effectively constrain the gradient consistency between the data distribution injected into adversarial perturbations and the generated distribution (*i.e.*, the distribution of generated relation matrices or node representations). Therefore, we replace the reconstruction loss in graph adversarial learning with the proposed gradient distribution consistency loss to circumvent the inaccurate prior distribution issue.

Contribution. Our main contributions are summarized as follows: (1) We propose a graph generative modeling-based training scheme, X-GGM, which can markedly improve the OOD generalization ability of existing VQA models while preserving their ID performance. (2) We propose a gradient distribution consistency loss, which can effectively alleviate the unstable gradient issue in graph adversarial learning by constraining the gradient consistency of the data distribution with adversarial perturbations and the generated distribution. (3) The baseline VQA model (LXMERT) trained with the proposed X-GGM scheme achieves state-of-the-art OOD performance while preserving the ID performance on two standard VQA OOD benchmarks, *i.e.*, VQA-CP v2 and GQA-OOD.

2 RELATED WORK

2.1 OOD Generalization in VQA

Training and testing under the independent and identically distributed (i.i.d) setting have resulted in the performance of most VQA models being highly affected by superficial correlations (*i.e.*, language biases and dataset biases) [1, 2, 20, 75]. Recently, evaluation on the out-of-distribution (OOD) setting [18, 24, 35, 61] has thus become an increasing concern for VQA. To improve the OOD generalization performance of VQA models, the prevailing methods target eliminating the language bias. Accordingly, current debiasing methods to VQA can be broadly divided into two groups, Known Bias-based [7, 10, 46] and Unknown Bias-based [11, 18, 59].

Known Bias-based methods consider the prior knowledge of language biases and design specific debiasing methods to reduce the biases explicitly existing in training set. Unknown Bias-based methods aim to remove the language bias or the answer distribution shift without the bias to be known in advance, which are more practical. In addition to considering extra human annotations [18, 53, 66] to balance datasets to reduce biases, most Unknown Bias-based methods leverage the adversarial training strategy [15, 18, 21, 44, 58, 61]. Particularly, VILLA [15] introduces adversarial perturbations into embedding space and utilizes large-scale adversarial training to improve the generalization ability. Similarly, the proposed X-GGM scheme injects adversarial perturbations into representation space and utilizes the adversarial learning strategy based on graph generative modeling to achieve OOD generalization and to mitigate language biases without prior knowledge of these biases.

2.2 Graph Generative Models

Graph Generative Modeling (GGM), aiming to learn to generate new graphs with certain desirable properties by observing existing graphs, has emerged in biomedical [13], social science [49], and graph representation learning [51, 65, 73]. Recent advances in deep generative models, especially VAE [37] and GAN [19], have developed towards the graph domain, inspiring many graph generative models, such as GAE [39], GraphVAE [56], GraphGAN [65], and Graphite [22]. These graph generative models follow the uniform framework that includes generative and discriminative models, limiting the scale of generated graphs. In order to handle the challenge of scalability, deep autoregressive models are utilized for graph generation, such as GraphRNN [71], GRANs [47], and GraphAF [54]. Furthermore, GRAM [34] introduces graph attention mechanism to enable the graph generative model scalability.

Recent approaches consider improving the generalization ability of graph generative models. You *et al.* [72] propose GraphCL, a contrastive learning-based framework, to learn robust graph representations. Pan *et al.* [51] encode the topological structure and node content in a graph to obtain compact graph representations by a novel adversarial graph embedding framework. Dai *et al.* [12] propose ANE, an Adversarial Network Embedding framework, to leverage the adversarial learning principle to regularize the representation learning, contributing to the learning stable and robust graph representation. Zheng *et al.* [77] propose DB-GAN, which implicitly bridges the graph and feature spaces by prototype learning, to learn more robust graph representation. The proposed X-GGM scheme considers generating both relationships between nodes and node representations during graph generative modeling to enhance the generalization ability of graph generative models.

2.3 Graph Construction in V+L Tasks

Graphs are non-Euclidean structured data, which can effectively represent relationships between nodes. Some recent works construct graphs for visual or linguistic elements in V+L tasks, such as VQA [16, 27, 43], VideoQA [28, 30, 79], Image Captioning [23, 70, 76], and Visual Grounding [31, 48, 69], to reveal relationships between these elements and obtain fine-grained semantic representations. These constructed graphs can be broadly grouped into three types: visual graphs between image objects/regions (*e.g.*, [70]),

linguistic graphs between sentence elements/tokens (e.g., [33]), and crossmodal graphs among visual and linguistic elements (e.g., [48]). In this work, we construct the visual graph for X-GGM.

3 PRELIMINARY

Taking the open-ended VQA task as a multi-class classification problem, the VQA model requires identifying the correct answer from a predefined set ($a \in \mathbb{A}$) of possible answers based on understanding the related question q and image I . Commonly, a VQA model (\mathcal{VQA}) can be divided into two modules: Cross-modality Representation ($\mathcal{VQA}_{\mathcal{R}}$) and Answer Classifier ($\mathcal{VQA}_{\mathcal{C}}$), which can be formulated by

$$\hat{a} = \mathcal{VQA}_{\mathcal{C}}(a|x), \quad \mathbf{x} = \mathcal{VQA}_{\mathcal{R}}(q, I), \quad (1)$$

where, $\mathcal{VQA}_{\mathcal{R}}$ is the crucial module of a VQA model, determining the representation ability of the VQA model. Therefore, the method aiming to achieve OOD generalization in VQA needs to improve the generalization performance while maintaining the representation ability of \mathbf{x} . In this paper, we consider two prevailing VQA models, i.e., transformer-based model (LXMERT [57]) and plain model (UpDn [3]), as our baseline VQA models for evaluating the OOD performance of the proposed X-GGM scheme.

LXMERT. LXMERT [57] is a classic transformer based on cross-modality pre-training, consisting of two single-modality encoders for visual and language modalities, respectively, and one cross-modality encoder for aligning entities across the two modalities. It can output a visual feature sequence $\{\mathbf{o}_n | \mathbf{o}_n \in \mathbb{R}^d, 1 \leq n \leq N_o\}$, a language feature sequence, and the cross-modality feature vector $\mathbf{x} \in \mathbb{R}^d$, where, N_o is the number of objects in one image, and \mathbf{o}_n is the n -th object feature vector. The visual feature sequence $\{\mathbf{o}_n\}$ and the cross-modality feature vector \mathbf{x} will be passed into the X-GGM scheme to improve the OOD generalization ability of \mathbf{x} by generatively modeling new relationships between objects and new node representations.

UpDn. Bottom-Up Top-Down model (UpDn) [3] is a typical attention based VQA model. For each image I , it utilizes an image encoder to output the sequence of object features: $\{\mathbf{o}_n | \mathbf{o}_n \in \mathbb{R}^d, 1 \leq n \leq N_o\}$. For each question, it utilizes a question encoder to output the sequence of language features. After that, both the object and language features are fed into an attention module to obtain the joint representation $\mathbf{x} \in \mathbb{R}^d$ for answer prediction. $\{\mathbf{o}_n\}$ and \mathbf{x} are the inputs of the X-GGM scheme.

4 GRAPH GENERATIVE MODELING

To improve the OOD generalization ability of \mathbf{x} while preserving its representation ability, we consider the nature attribute of compositional generalization implicit in the information aggregation of graph nodes, and propose a Graph Generative Modeling-based training scheme (X-GGM). The overall process of training a baseline VQA model with the X-GGM scheme is shown in Algorithm 1, consisting of two parts: Graph Generative Modeling (X-GGM) and Baseline Model Update (BMU). Once $\mathcal{VQA}_{\mathcal{R}}$ yields the cross-modality representation \mathbf{x} and the sequence of visual feature vectors $\{\mathbf{o}_n | \mathbf{o}_n \in \mathbb{R}^d, 1 \leq n \leq N_o\}$, X-GGM will update relationships between objects and representations of objects by

Algorithm 1 Training a VQA Model with X-GGM

```

1: function X-GGM( $I, q, a, R_{GT}$ )
2:    $\{\mathbf{o}_n, 1 \leq n \leq N_o\}, \mathbf{x} \leftarrow \mathcal{VQA}_{\mathcal{R}}(I, q)$ 
3:    $cond \sim U[0, 1]$ 
4:   if  $cond \leq \eta$  then                                      $\triangleright$  execute R-GGM
5:      $R_0 \leftarrow R_{INIT}(\mathbf{x}, \sigma)$ 
6:      $R_g, \{\bar{v}_1, \dots, \bar{v}_{N_k}\} \leftarrow R_{GEN}(\{\mathbf{o}_n\}, R_0)$ 
7:      $p_a \leftarrow \mathcal{VQA}_{\mathcal{C}}(\mathbf{x}, \bar{v}_{N_k})$ 
8:      $\mathcal{L} \leftarrow R_{LEARN}(R_g, R_{GT}, p_a)$ 
9:   else                                                    $\triangleright$  execute N-GGM
10:     $\{v_i, 1 \leq i \leq N_o\}_0 \leftarrow N_{INIT}(\mathbf{x}, \sigma)$ 
11:     $V_g, \{\bar{v}_1, \dots, \bar{v}_{N_k}\} \leftarrow N_{GEN}(\{v_i\}_0, R_{GT})$ 
12:     $p_a \leftarrow \mathcal{VQA}_{\mathcal{C}}(\mathbf{x}, \bar{v}_{N_k})$ 
13:     $\mathcal{L} \leftarrow N_{LEARN}(V_g, \{\mathbf{o}_n\}, p_a)$ 
14:   end if
15: end function
1: function BMU( $I, q, a$ )
2:    $p_a \leftarrow \mathcal{VQA}(I, q, a)$                                 $\triangleright$  training baseline model
3: end function

```

Graph Relation Generative Modeling (R-GGM) and Graph Representation Generative Modeling (N-GGM) in each training update¹. In the following, we first introduce the predefined object-relation graph and then detail R-GGM and N-GGM.

4.1 Graph Construction

For the X-GGM scheme, we construct an object-relation graph using objects in one image as graph nodes. Specifically, the object-relation graph can be formulated as $\mathcal{G} = (\mathcal{V}, \mathbf{A}, \mathbf{R})$, where $\mathcal{V} = \{v_1, \dots, v_{N_o}\}$ is a set of nodes with $|\mathcal{V}| = N_o$. \mathbf{A} is the adjacency matrix with $a_{i,j} \in \mathbf{A}$ marking whether there is an edge between node v_i and v_j , and \mathbf{R} is a relation matrix describing the coherence between nodes. The constructed graph \mathcal{G} is a fully-connected graph, meaning that the adjacency matrix \mathbf{A} is an all-ones matrix. Therefore, we omit \mathbf{A} in \mathcal{G} for conciseness in following sections.

To determine the ground-truth (GT) of relation matrix R_{GT} utilizing in R-GGM, we compute the cosine similarity between object-class embeddings $\{c_n | c_n \in \mathbb{R}^d, 1 \leq n \leq N_o\}$ and object-attribute embeddings $\{a_n | a_n \in \mathbb{R}^d, 1 \leq n \leq N_o\}$. These embeddings (i.e., c_n and a_n) are obtained by a pre-trained BERT model [14]. Practically, the similarity computations are random combinations of object-classes and object-attributes in one image, which will breed new combinations. In N-GGM, the object feature \mathbf{o}_n yielded by $\mathcal{VQA}_{\mathcal{R}}$ serves as the GT of the i -th node representation (i.e., $v_{GT,i} = \mathbf{o}_n$).

4.2 Graph Relation Generative Modeling

Graph Relation Generative Modeling (R-GGM) consists of three stages: initializing relation matrix utilizing \mathbf{x} and Gaussian noise (RINIT), Graph Relation Matrix Generation (RGEN), and Adversarial Learning of Relation (RLEARN).

Initializing Relation Matrix (RINIT). The graph \mathcal{G} is an undirected graph with N_o nodes. Therefore, the relation matrix $\mathbf{R} \in$

¹Since the explicit relation triplets between objects are challenging to obtain, this paper operates the relation matrix and node representations instead of the adjacency matrix to achieve implicit recompositions.

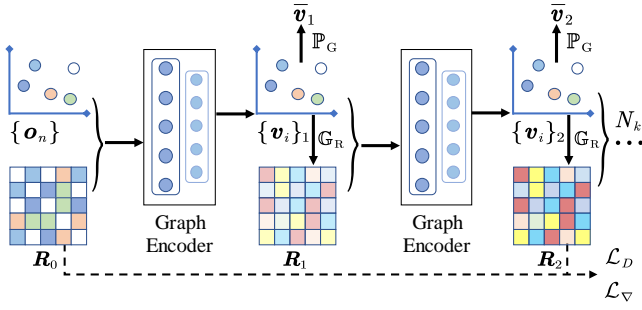


Figure 3: Graph Relation Generation. \mathbb{P}_G indicates the average pooling of node representations, and \mathbb{G}_R denotes generating relation matrix by Eq. (6).

$\mathbb{R}^{N_o \times N_o}$ is symmetric, meaning that only the upper triangular elements without diagonal elements (always 1) need to be initialized. Specifically, we first transform \mathbf{x} into a vector $\mathbf{r} \in \mathbb{R}^{N_o(N_o-1)/2}$ by

$$\mathbf{r} = \text{Sigmoid}(\mathbf{W}_r \mathbf{x} + \mathbf{b}_r), \quad (2)$$

where, $\mathbf{W}_r \in \mathbb{R}^{N_o(N_o-1)/2 \times d}$ is the transformation matrix, the learnable bias \mathbf{b}_r has same size as \mathbf{r} , and Sigmoid denotes the Sigmoid activation function. Subsequently, we inject the adversarial perturbation (i.e., Gaussian noise) to \mathbf{r} and make $\hat{\mathbf{r}} \sim p_\sigma(\hat{\mathbf{r}}|\mathbf{r})$:

$$p_\sigma(\hat{\mathbf{r}}|\mathbf{r}) = \frac{1}{\sqrt{2\pi}\sigma} \exp\left\{-\frac{(\hat{\mathbf{r}} - \mathbf{r})^2}{2\sigma^2}\right\}, \quad (3)$$

where σ is the standard deviation of Gaussian noise. Finally, we sequentially fill the upper triangular part (\mathbf{R}_0^+) of \mathbf{R}_0 with the elements of $\hat{\mathbf{r}}$, and obtain the initial relation matrix by $\mathbf{R}_0 = \mathbf{R}_0^+ + (\mathbf{R}_0^+)^T$.

Relation Matrix Generation (RGEN). The detailed process of RGEN is shown in Figure. 3, which can be accomplished in N_k iterations. Before the iteration beginning, node representations of the graph \mathcal{G} are initialized by the corresponding object feature vector, i.e., $\mathbf{v}_i = \mathbf{o}_n$ ($i = n$). In the k -th ($1 \leq k \leq N_k$) iteration, node representations $\mathbf{V}_{k-1} = \{\mathbf{v}_i\}_{k-1}$ and the relation matrix \mathbf{R}_{k-1} yielded by Graph Encoder in the $(k-1)$ -th iteration are first fed into the k -th Graph Encoder and served as inputs (i.e., $\mathbf{V}_k^{(0)} = \mathbf{V}_{k-1} \in \mathbb{R}^{N_o \times d}$ and $\mathbf{R}_k^{(0)} = \mathbf{R}_{k-1} \in \mathbb{R}^{N_o \times N_o}$). Subsequently, the node representations are encoded by Graph Encoder, which is essentially a GCN [38] with N_l -layers. Specifically, the node representations in the l -layer of Graph Encoder can be updated with

$$\mathbf{V}_k^{(l+1)} = \text{Sigmoid}((\mathbf{R}_k^{(0)} \mathbf{V}_k^{(l)} \mathbf{W}_k^{(l)} + \mathbf{b}_k^{(l)}), \quad (4)$$

where, $\mathbf{W}_k^l \in \mathbb{R}^{N_o \times d \times d}$ is spanned by N_o matrices of feature transformation, and $\mathbf{b}_k^l \in \mathbb{R}^{N_o \times d}$ is the learnable bias for the transformation. After that, we assemble the input and the output of each layer in Graph Encoder to obtain the final output \mathbf{V}_k of the k -th iteration:

$$\mathbf{V}_k = \sum_{l=0}^{N_l} \text{ReLU}(\mathbf{V}_k^{(l)} \mathbf{W}_a + \mathbf{b}_a), \quad (5)$$

where, ReLU denotes the ReLU activation function, $\mathbf{W}_a \in \mathbb{R}^{N_o \times d \times d}$ and $\mathbf{b}_a \in \mathbb{R}^{N_o \times d}$ are the weight and bias for node feature transformation, respectively. Finally, the relation matrix is generated using the final node representations \mathbf{V}_k by

$$\mathbf{R}_k = \text{Sigmoid}(\mathbf{V}_k \mathbf{V}_k^T). \quad (6)$$

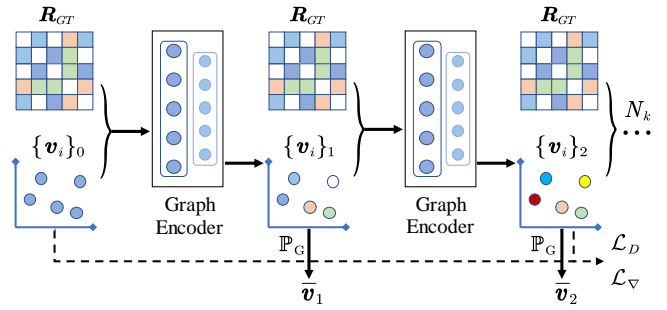


Figure 4: Graph Representation Generation. \mathbb{P}_G is an average operation of node representations.

We utilize the output of the last iteration as the final generated relation matrix, that is, $\mathbf{R}_g = \mathbf{R}_{N_k}$. In addition, we average node representations $\{\mathbf{v}_i, 1 \leq i \leq N_o\}_k$ to derive the graph representation $\bar{\mathbf{v}}_k$ in the k -th iteration.

Adversarial Learning of R-GGM (RLEARN). When initializing the relation matrix in the stage of RINIT, we find that the process of R-GGM introducing adversarial perturbations is similar to that of Denoising AutoEncoder [64]. From the works [5, 45], we know that the optimal Denoising AutoEncoder for additive white Gaussian noise (AWGN) can be explicitly calculated, which is related to the gradient of the data distribution after adding noises. Practically, the logarithmic gradient of the data distribution with adversarial perturbations can be deduced from Eq. (3):

$$\nabla_{\hat{\mathbf{r}}} \log p_\sigma(\hat{\mathbf{r}}|\mathbf{r}) = -\frac{(\hat{\mathbf{r}} - \mathbf{r})^2}{\sigma^2}. \quad (7)$$

After obtaining $\nabla_{\hat{\mathbf{r}}} \log p_\sigma(\hat{\mathbf{r}}|\mathbf{r})$, we can compute the gradient of log-likelihood estimation, i.e., $\nabla_{\mathbf{r}} \log p_g(\mathbf{r})$, of elements in the generated relation matrix \mathbf{R}_g to constrain the gradient distribution consistency between the generated relation matrix \mathbf{R}_g and the pre-derived similarity matrix \mathbf{R}_{GT} . Therefore, the gradient distribution consistency loss can be defined as

$$\mathcal{L}_\nabla \triangleq \mathbb{E} \left[\left\| \nabla_{\mathbf{r}} \log p_g(\mathbf{r}) - \nabla_{\hat{\mathbf{r}}} \log p_\sigma(\hat{\mathbf{r}}|\mathbf{r}) \right\|_2^2 \right]. \quad (8)$$

In addition to constraining the gradient distribution consistency, we further utilize KL-Divergence to measure the distance between the generated distribution $p_g(\mathbf{r})$ and the raw data distribution $p_{data}(\mathbf{r})$, where p_g and p_{data} denote probability distributions of elements in matrix \mathbf{R}_g and \mathbf{R}_{GT} , respectively. The distance measure loss of training our R-GGM can be formulated by

$$\mathcal{L}_D = \text{KL}(p_g \| p_{data}) + \text{KL}(p_{data} \| p_g), \quad (9)$$

where, $\text{KL}(p \| q) = \mathbb{E}_{\mathbf{r} \sim p} [\log p(\mathbf{r}) - \log q(\mathbf{r})]$.

Besides the adversarial losses (i.e., \mathcal{L}_∇ and \mathcal{L}_D), we compute the BCE loss (\mathcal{L}_{BCE}) of the VQA task by adding \mathbf{x} (the original cross-modality representation) and $\bar{\mathbf{v}}_{N_k}$ (the graph representation yielded by the last iteration in RGEN) and passing the value into $\mathcal{VQA}_{\mathcal{C}}$ to derive the likelihood estimation of answer distribution p_a .

In summary, the total loss of training R-GGM can be formulated by

$$\mathcal{L} = \alpha \mathcal{L}_\nabla + \beta \mathcal{L}_D + \mathcal{L}_{\text{BCE}}, \quad (10)$$

where, α and β are weighted coefficients.

Table 1: Statistics of VQA-CP v2 and GQA-OOD.

Dataset	Image					Question					Year
	Train	Val	OOD Test	ID Test	Total	Train	Val	OOD Test	ID Test	Total	
VQA-CP v2 [2]	119,107	31,976	89,437	32,266	272,786	388,735	38,802	179,928	40,000	647,465	2018
GQA-OOD [35]	72,140	9,406	330	365	82,241	943,000	51,045	1,063	1,733	996,841	2020

4.3 Graph Representation Generative Modeling

Graph Representation Generative Modeling (N-GGM) is similar to R-GGM, which can also be implemented in three stages: initializing node representations with \mathbf{x} and Gaussian noise (NINIT), Graph Node Representation Generation (NGEN), and Adversarial Learning of Node Representation (NLEARN).

Initializing Node Representations (NINIT). To obtain the N_o initial node representations of the graph \mathcal{G} , we first span \mathbf{x} to $[\mathbf{x}, \dots, \mathbf{x}] \in \mathbb{R}^{N_o \times d}$, and utilize a fully-connected layer (\mathcal{M}_{FC}) to increase the variability of node representations:

$$\mathbf{V}_x = \mathcal{M}_{FC}([\mathbf{x}, \dots, \mathbf{x}]), \mathbf{V}_x \in \mathbb{R}^{N_o \times d}, \quad (11)$$

where, $\mathbf{V}_x = \{v_{i,x} | v_{i,x} \in \mathbb{R}^d\}$, $1 \leq i \leq N_o$. After that, we inject adversarial perturbations to \mathbf{V}_x , and make the sampled feature vector $\hat{v}_{i,x}$ of the i -th element in \mathbf{V}_x satisfy the noise prior distribution $p_\sigma(\hat{v}_{i,x} | v_{i,x})$:

$$p_\sigma(\hat{v}_{i,x} | v_{i,x}) = \frac{1}{\sqrt{2\pi}\sigma} \exp\left\{-\frac{(\hat{v}_{i,x} - v_{i,x})^2}{2\sigma^2}\right\}. \quad (12)$$

Finally, the initial node representations of the graph \mathcal{G} can be obtained by $\mathbf{V}_0 = \hat{\mathbf{V}}_x = [\hat{v}_{0,x}, \dots, \hat{v}_{N_o,x}]$.

Node Representation Generation (NGEN). The details of NGEN are shown in Figure 4. In the k -th iteration, the node representations $\mathbf{V}_{k-1} = \{v_i, 1 \leq i \leq N_o\}_{k-1}$ generated by Graph Encoder in the $(k-1)$ -th iteration and the predefined GT relation matrix \mathbf{R}_{GT} are first passed into the k -th Graph Encoder to update the node representations of each layer. After that, the final output of the k -th Graph Encoder \mathbf{V}_k can be obtained by Eq. (5). The architecture of Graph Encoder in N-GGM is the same as that in R-GGM. We utilize the output of the last iteration as the generated node representations, *i.e.*, $\mathbf{V}_g = \mathbf{V}_{N_k}$. Besides, in each iteration, we average N_o node representations and yield the graph representation \bar{v}_k .

Adversarial Learning of N-GGM (NLEARN). The total loss \mathcal{L} of training N-GGM is also a weighted sum of \mathcal{L}_∇ , \mathcal{L}_D , and \mathcal{L}_{BCE} . Specifically, the gradient distribution consistency loss \mathcal{L}_∇ is defined as the distance between the distribution gradient of the initial node representations after adding Gaussian noise ($\hat{\mathbf{V}}_x$) and the log-likelihood estimation of generated node representations (\mathbf{V}_g). \mathcal{L}_D is the KL-Divergence loss between the distribution of generated node representations (\mathbf{V}_g) and the distribution of the raw node representations ($\{\mathbf{o}_n\}$) yielded by $\mathcal{VQA}\mathcal{A}\mathcal{R}$. The VQA classification loss \mathcal{L}_{BCE} is the same as the corresponding term in Eq. (10).

5 EXPERIMENTS

In this section, we evaluate the effectiveness of X-GGM key components and compare the proposed X-GGM scheme with state-of-the-art approaches on two standard VQA OOD benchmarks, *i.e.*, VQA-CP v2 [2] and GQA-OOD [35]. Table 1 reports the statistics of experimental datasets.

Table 2: Ablation studies on R-GGM and N-GGM with different combinations of \mathcal{L}_D and \mathcal{L}_∇ (More results are shown in Table 6 of the Appendix). \uparrow (\downarrow) indicates the higher (lower) the better. LX. means the Baseline, *i.e.*, LXMERT.

S/N	R-GGM		N-GGM		VQA-CP v2			GQA-OOD		
	\mathcal{L}_∇	\mathcal{L}_D	\mathcal{L}_∇	\mathcal{L}_D	OOD \uparrow	ID \uparrow	Gap \downarrow	Tail \uparrow	Head \uparrow	$\Delta\downarrow$
LX.	—				59.98	65.21	5.23	49.80	57.70	15.90
#1	✓	✓			63.84	66.41	2.57	51.39	56.93	10.77
#2			✓	✓	62.90	65.57	2.67	51.27	57.30	11.76
#3	✓		✓		63.75	66.03	2.28	51.65	57.13	10.61
#4		✓		✓	62.73	65.99	3.26	51.27	57.19	11.54
#5	✓	✓	✓	✓	64.33	66.92	2.59	52.47	57.51	9.59

5.1 Experimental Settings

5.1.1 Evaluation Benchmarks.

VQA-CP v2. It is the reorganization of the training and validation sets of VQA v2.0 [55]. To evaluate the OOD generalization performance of existing VQA models, Agrawal *et al.* [2] construct VQA-CP v2 by ensuring that the answer distribution of per question type in the test set and the training set is different. The original VQA-CP v2 only consists of the test set (about 98K images, 220K questions, and 2.2M answers) and the training set (about 121K images, 438K questions, and 4.4M answers). That is, the benchmark does not have an official validation set.

GQA-OOD. It is a fine-grained restructuring of GQA [29], which obtains the validation and test sets by introducing answer distribution shifts into the validation and test sets of GQA. However, GQA-OOD shares the same training set with GQA. The GQA-OOD benchmark provides four metrics. 1) **Tail**: accuracy on OOD samples (*i.e.*, samples of the tail of the answer class distribution), 2) **Head**: accuracy on in-domain (ID) samples (*i.e.*, samples from the head distribution), 3) **All**: overall accuracy on all test samples, and 4) $\Delta(\%) = (\text{head} - \text{tail}) / \text{tail}$: a new evaluation protocol proposed by Kervadec *et al.* [35] to illustrate how much is the error prediction imbalanced between frequent and rare answers.

5.1.2 Experimental Details.

Data Preprocessing. As Teney *et al.* [61] discussed, there are several pitfalls in evaluating VQA models under the OOD setting on VQA-CP v2, especially using the OOD test set for model selection and evaluating the ID performance of a VQA model after re-training the model on VQA v2.0 [55]. Therefore, following recent works [11, 58–60], we re-split VQA-CP v2. Specifically, we reserve 40k random samples from the train set to evaluate the in-domain (ID) performance and 40k random instances from the test set for model selection. Besides, the bottom-up attention Faster R-CNN [3]

pre-trained on Visual Genome [40] is utilized to obtain object class and attribute in the image for the two datasets.

Implementation Details. For X-GGM, we set the number N_o of nodes in \mathcal{G} to 36 and the standard feature dimensionality d to 768. The standard deviation σ in Eq. (3) is 1.0. The threshold η in Algorithm 1 are 0.8 and 0.5 for VQA-CP v2 and GQA-OOD, respectively. The total step N_k of X-GGM is 2, and the layer N_l of the encoder in each step is 2. The weight coefficients α and β in Eq. (10) are 6 and 72 for R-GGM, and 6.6 and 0.17 for N-GGM. All experiments are implemented on one NVIDIA GTX2080 12GB GPU for 5 epochs with a batch size of 128 and a learning rate of 1e-6.

5.2 Ablation Studies

We conduct ablation studies on key components of X-GGM using LXMERT as the baseline VQA model². Considering the discovery in work [61], *i.e.*, the questions with yes/no/number answers on VQA-CP v2 are easier to game, for a fairer comparison, we train all models on VQA-CP v2 “All”. But, we select the best model and focus the model analysis on VQA-CP v2 “other”.

5.2.1 Effectiveness of Key Components.

R-GGM / N-GGM / X-GGM vs. Baseline. To improve the OOD generalization ability of the cross-modality representation \mathbf{x} yielded by $\mathcal{VQA}_{\mathcal{R}}$, besides training the baseline VQA model using the full X-GGM scheme, R-GGM and N-GGM can also work independently. Therefore, we consider comparisons between the ablated components (#1, #2, #5) and the Baseline, *i.e.*, LXMERT (LX.) in Table 2 to evaluate the respective effects of R-GGM, N-GGM, and X-GGM. Specifically, \blacktriangleright LX. vs. #1 (only using R-GGM in the training process). \blacktriangleright LX. vs. #2 (only using N-GGM in the training process). \blacktriangleright LX. vs. #5 (using the full X-GGM scheme that executes R-GGM and N-GGM at a ratio of η in the training process). Table 2 shows the results on VQA-CP v2 “Other” and GQA-OOD. LX. vs. #5 demonstrates the effectiveness of X-GGM. LX. vs. #1 / #2 illustrates that the single R-GGM / N-GGM can also effectively improve the OOD generalization performance of the baseline VQA model.

R-GGM / N-GGM vs. X-GGM. In each training iteration, X-GGM randomly executes R-GGM or N-GGM to improve the OOD generalization ability of the baseline VQA model. To explore the importance of R-GGM and N-GGM to the full training scheme (X-GGM), as shown in Table 2 (#1, #2, #5), we conduct the following comparisons: \blacktriangleright #1 vs. #5, and \blacktriangleright #2 vs. #5. The results in Table 2 indicate that R-GGM is more effective than N-GGM for the X-GGM scheme in boosting the OOD performance of the baseline VQA model (LXMERT) on both VQA-CP v2 “Other” and GQA-OOD. This is mainly because the gradient instability caused by the noise introduction in N-GGM is larger than that in R-GGM. Specifically, the noise vector dimensions introduced into R-GGM and N-GGM are $N_o(N_o - 1)/2 = 630$ and $N_o \times d = 27,648$, respectively.

Gradient Distribution Consistency Loss. To evaluate the effectiveness of the gradient distribution consistency loss \mathcal{L}_{∇} in alleviating the unstable gradient issue, we compare the respective effects of \mathcal{L}_{∇} and \mathcal{L}_D . The KL-Divergence loss \mathcal{L}_D is also an adversarial

²Pre-trained transformers usually have smaller ID/OOD generalization gaps than previous plain models [26]. Considering that improving the OOD performance of transformer-based methods is more difficult than plain methods, we utilize a transformer-based model as the baseline to conduct our ablation studies.

Table 3: Comparisons between different variants of Graph Encoder (GEnc.) with N_l layers.

GEnc.	N_l	VQA-CP v2			GQA-OOD		
		OOD \uparrow	ID \uparrow	Gap \downarrow	Tail \uparrow	Head \uparrow	$\Delta\downarrow$
LX.	—	59.98	65.21	5.23	49.80	57.70	15.90
GCN	1	64.10	66.70	2.60	51.65	57.24	10.83
	2	64.33	66.92	2.59	52.47	57.51	9.59
GIN	1	63.62	66.24	2.62	50.99	57.08	11.93
	2	63.83	66.39	2.56	51.27	57.30	11.76
GAT	1	63.94	66.40	2.46	51.65	57.71	11.73
	2	63.94	66.45	2.51	50.99	56.90	11.59

loss. The experimental settings are shown in Table 2 (#3, #4, #5). More specifically, \triangleright #3: only using \mathcal{L}_D as the adversarial loss to train the baseline VQA model (LXMERT) with the X-GGM scheme, \triangleright #4: only using \mathcal{L}_{∇} as the adversarial loss to train the baseline VQA model with the X-GGM scheme, and \triangleright #5: using a weighted sum of \mathcal{L}_{∇} and \mathcal{L}_D as the adversarial loss to train the baseline VQA model with the X-GGM scheme. The comparisons between #3, #4, and #5 on VQA-CP v2 “Other” and GQA-OOD in Table 2 illustrate that both \mathcal{L}_D and \mathcal{L}_{∇} are effective for training the baseline VQA model with the X-GGM scheme. However, \mathcal{L}_{∇} performs better than \mathcal{L}_D , demonstrating the effectiveness of \mathcal{L}_{∇} in alleviating unstable gradient updates in graph adversarial learning.

5.2.2 Variants of Graph Encoder.

In the proposed X-GGM scheme, Graph Encoder is a general block utilized to aggregate node information and encode relationships between nodes. That is, architecture differences between different Graph Encoders can not markedly affect the performance of X-GGM to OOD generalization. To demonstrate that the X-GGM scheme is robust for different variants of Graph Encoder, we consider three prevailing Graph Neural Networks (*i.e.*, GCN [38], GIN [67], and GAT [63]) and set the number of their layers N_l to 1 and 2. From the results on VQA-CP v2 “Other” and GQA-OOD shown in Table 3, we can observe that there is only a slight difference between the OOD performance of different Graph Encoder variants. However, all of these variants have achieved dramatic improvements in OOD performance compared with the baseline VQA model (LXMERT). The results demonstrate that X-GGM is agnostic to Graph Encoder and is robust for different Graph Encoders.

5.2.3 Hyperparameter.

Ratio of R-GGM and N-GGM η . The threshold η in Algorithm 1 determines the ratio of R-GGM and N-GGM executed in each training iteration. To analyze the influence of η for X-GGM improving the OOD performance, we conduct some ablated experiments on different values of η , *i.e.*, $\eta \in \{0.1, 0.2, \dots, 0.9\}$. Results on VQA-CP v2 “Other” and GQA-OOD are shown in Figure 5 (a) and (b), respectively. We observe that the baseline VQA model (LXMERT) trained with the proposed X-GGM scheme can achieve the best OOD performance on VQA-CP v2 “Other” and GQA-OOD when $\eta = 0.8$ and $\eta = 0.5$, respectively. The average gains of the OOD performance on VQA-CP v2 “Other” and GQA-OOD are $+3.76_{\pm 0.36}$ and $+1.54_{\pm 0.59}$, respectively. Comparing the OOD performance gains

Table 4: Comparisons with UB-based debiasing methods on VQA-CP v2 (full comparisons with state-of-the-arts are reported in Table 7 of the Appendix). †: methods using additional manually annotated data, *: results from our reimplementation using the official released code, —: not reported.

Method	VQA-CP v2 (OOD Test) ↑				VQA-CP v2 (ID Test) ↑				Gap ↓			
	All	Yes/No	Num.	Other	All	Yes/No	Num.	Other	All	Yes/No	Num.	Other
Unshuffling [59]	42.39	47.72	14.43	47.24	—	—	—	—	—	—	—	—
Unshuffling+CF [58]	40.60	61.30	15.60	46.00	63.30	79.40	45.50	53.70	22.70	18.10	29.90	7.70
Unshuffling+CF+GS [58]	46.80	64.50	15.30	45.90	62.40	77.80	43.80	53.60	15.60	13.30	28.50	7.70
UpDn [3]	38.82	42.98	12.18	43.95	64.73	79.45	49.59	55.66	25.91	36.47	37.32	11.71
+ Top answer masked [61]	40.61	82.44	27.63	22.26	30.90	44.12	5.00	20.85	9.71	38.32	22.63	1.41
+ AdvReg [21]	36.33	59.33	14.01	30.41	50.63	67.39	38.81	38.37	14.30	8.06	24.80	7.96
+ GRL [21]	42.33	59.74	14.78	40.76	56.90	69.23	42.50	49.36	14.57	9.49	27.72	8.60
+ RandImg ($\lambda=12$) [61]	55.37	83.89	41.60	44.20	54.24	64.22	34.40	50.46	1.13	19.67	7.20	6.26
+ RandImg ($\lambda=5$) [61]	51.15	75.06	24.30	45.99	59.28	70.66	43.06	53.40	8.13	4.40	18.76	7.41
+ MUTANT† [18]	61.72	88.90	49.68	50.78	—	—	—	—	—	—	—	—
+ X-GGM	45.71	43.48	27.65	52.34	67.16	83.74	48.26	56.91	21.45	40.26	20.61	4.57
LXMERT* [57]	63.90	80.45	46.58	59.98	75.57	91.39	59.83	65.21	11.67	10.94	13.25	5.23
+ MUTANT† [18]	69.52	93.15	67.17	57.78	—	—	—	—	—	—	—	—
+ VILLA* [15]	48.06	42.66	18.97	58.89	75.85	90.40	60.02	66.66	27.79	47.74	41.05	7.77
+ X-GGM	66.95	78.91	53.63	64.33	75.88	90.18	60.06	66.92	8.93	11.27	6.43	2.59

(w.r.t. the baseline VQA model) with the standard deviations of the OOD performance, we can consider the performance fluctuation is slight, demonstrating the robustness of the X-GGM scheme to the hyperparameter η .

5.3 Comparisons with State-of-the-Arts

To evaluate the OOD and ID performance of baseline VQA models trained with the proposed X-GGM scheme, we compare them with state-of-the-art methods on VQA-CP v2 and GQA-OOD.

5.3.1 Performance on VQA-CP v2.

Setting. X-GGM is a training scheme for improving the OOD generalization ability of baseline VQA models while preserving the ID performance, which alleviates the language bias in VQA to some extent without the bias being known in advance. Therefore, according to whether debiasing methods need to know the bias existing on the datasets beforehand, we group them into two types. (1) Known Bias-based (KB-based) methods, such as LMH [10], LRS [25], and LMH-MFE [17]. (2) Unknown Bias-based (UB-based) methods, such as MCE [11], MUTANT [18], Unshuffling [59], and VILLA [15]. Particularly, VILLA [15] utilizes the adversarial training strategy that introduces noises into representation space to improve model generalization ability. The strategy of injecting adversarial perturbations into representation space inspired our work. Therefore, we reimplement VILLA [15] on VQA-CP v2 for a fairer comparison. On VQA-CP v2, we utilize LXMERT and UpDn as baseline VQA models and mainly compare the proposed X-GGM scheme with UB-based methods (more comparisons with state-of-the-art methods are shown in the Appendix). As with ablation study, we implement our experiments on VQA-CP v2 “All” but focus comparisons on “Other”, which can better evaluate the ability of approaches to OOD generalization than “Yes/No” and “Num.”.

Results. Comparisons are reported in Table 4. As shown in the table, facilitated by the proposed X-GGM scheme, the baseline VQA

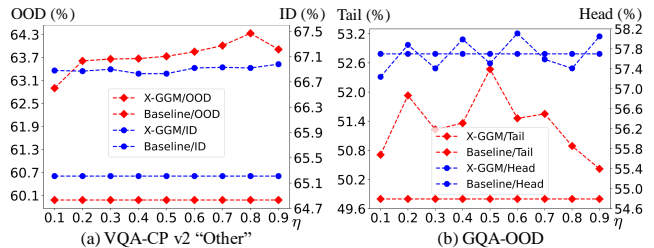


Figure 5: Ablation studies on the hyperparameter η . (a) OOD and ID accuracies of our method (X-GGM) and the Baseline (LXMERT) on VQA-CP v2 “Other”. (b) OOD (Tail) and ID (Head) accuracies on GQA-OOD.

model (LXMERT) achieves state-of-the-art OOD and ID performance on VQA-CP v2 “Other”. Besides, compared with all methods utilized UpDn as the baseline VQA model, our method also gains the best OOD and ID performance on “Other”. These results demonstrate the X-GGM scheme is effective for a VQA model to generalize to out-of-distribution samples while preserving its ID performance.

5.3.2 Performance on GQA-OOD.

Settings. Except for LMH [10] and LM [10], the other methods listed in Table 5 are UB-based and can be further grouped into plain models (models in the third row of Table 5, e.g., BAN4 [36] and MMN [8]) and transformer-based models (models in the fourth row of Table 5 like MCAN [74] and VILLA [15]). We utilize LXMERT and UpDn as baseline VQA models, and compare the proposed X-GGM scheme with all existing methods on GQA-OOD. Specifically, RUBi [6], LMH [10] and LM [10] utilize UpDn as their baseline model. VILLA [15] and MANGO [44] use LXMERT as the baseline VQA model. We also reimplement VILLA on GQA-OOD.

Table 5: Comparisons with state-of-the-arts on GQA-OOD.

Method	Metrics (%)			
	All \uparrow	Tail \uparrow	Head \uparrow	Δ \downarrow
Plain Models				
BAN4 [36]	50.20	47.20	51.90	9.90
MMN [8]	52.70	48.00	55.50	15.60
UpDn [3]	46.40	42.10	49.10	16.60
+ LMH [10]	33.10	30.80	34.50	12.00
+ LM [10]	34.50	32.20	35.90	11.50
+ RUBi [6]	38.80	35.70	40.80	14.30
+ X-GGM	48.41	45.99	49.90	8.51
Transformer-based Models				
MCAN [74]	50.80	46.50	53.40	14.80
MANGO ³ [44]	56.40	51.27	59.55	16.15
LXMERT [57]	54.60	49.80	57.70	15.90
+ VILLA* [15]	54.47	49.95	57.24	14.59
+ MANGO [44]	54.94	—	—	—
+ X-GGM	55.59	52.47	57.51	9.59

Results. From the comparisons in Table 5, we can observe that benefiting from the OOD generalization ability of X-GGM, the baseline VQA model (LXMERT) trained with our scheme outperforms all other methods on GQA-OOD on the metric **Tail**. Although the ID performance (Head) drops by 0.19 relative to the baseline VQA model, it is far smaller than the OOD performance improvement (2.67). Besides, the baseline VQA model (UpDn) trained with the X-GGM scheme also outperforms these methods utilized UpDn as the baseline VQA model on all metrics, especially on **Tail**. These results demonstrate the ability of the proposed X-GGM scheme to OOD generalization and ID preserving. Unfortunately, the OOD performance improvement on GQA-OOD is not as obvious as that on VQA-CP v2. It likely because questions of GQA-OOD are semantic compositionality. The syntax-complex questions weaken the representation ability of x while X-GGM also does not explicitly leverage the structured representation of question to enhance x .

5.4 Qualitative Examples

To qualitatively illustrate the effectiveness of the X-GGM scheme in improving the OOD performance of baseline VQA models, we show some prediction examples from the OOD test sets of VQA-CP v2 and GQA-OOD. As shown in Figure 6, the Baseline (*i.e.*, LXMERT) is prone to utilize in-domain answers (*e.g.*, *eating* and *sitting*) to answer out-of-distribution questions. In contrast, the Baseline after being trained with the proposed X-GGM scheme can yield out-of-distribution answers, such as *brushing teeth* and *posing* in the first row of Figure 6, demonstrating the ability of X-GGM to OOD generalization. More predictions and visualization of the generated relation matrices are shown in Figure 7-8 of the Appendix.

6 CONCLUSION

In this paper, we proposed a Graph Generative Modeling-based scheme, X-GGM, to improve the OOD generalization ability of baseline VQA models while preserving the ID performance. Specifically, the X-GGM scheme randomly executes R-GGM or N-GGM

³using UNITER [9] as the baseline VQA model.

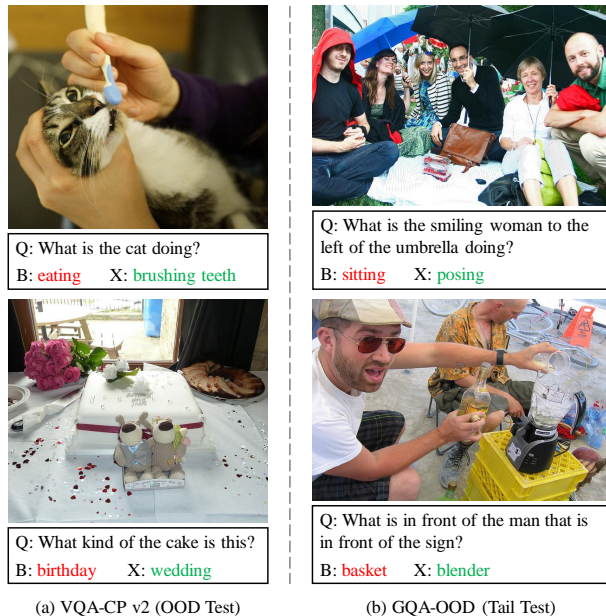


Figure 6: Qualitative examples from the OOD test set of VQA-CP v2 and GQA-OOD respectively provided by the Baseline (B), *i.e.*, LXMERT, and the Baseline trained with the X-GGM scheme (X). The wrong and correct answers are highlighted in red and green, respectively.

to generate a new relation matrix or new node representations to enable the baseline VQA model to generalize to out-of-distribution samples. Besides, to alleviate the unstable gradient issue in graph adversarial learning, we propose a gradient distribution consistency loss to constrain the derivative of data distribution with adversarial perturbations and generated distribution. We evaluate the effectiveness of X-GGM components by extensive and ablative experiments. The baseline VQA model (LXMERT) trained with the proposed X-GGM scheme achieves state-of-the-art OOD performance on two VQA OOD benchmarks while preserving the ID performance.

ACKNOWLEDGMENTS

This work was supported by the NSFC Grants 61773312, 62088102.

REFERENCES

- [1] Aishwarya Agrawal, Dhruv Batra, and Devi Parikh. 2016. Analyzing the Behavior of Visual Question Answering Models. In *EMNLP*. 1955–1960.
- [2] Aishwarya Agrawal, Dhruv Batra, Devi Parikh, and Aniruddha Kembhavi. 2018. Don’t just assume; look and answer: Overcoming priors for visual question answering. In *CVPR*. 4971–4980.
- [3] Peter Anderson, Xiaodong He, Chris Buehler, Damien Teney, Mark Johnson, Stephen Gould, and Lei Zhang. 2018. Bottom-up and top-down attention for image captioning and visual question answering. In *CVPR*. 6077–6086.
- [4] Stanislaw Antol, Aishwarya Agrawal, Jiasen Lu, Margaret Mitchell, Dhruv Batra, C Lawrence Zitnick, and Devi Parikh. 2015. Vqa: Visual question answering. In *CVPR*. 2425–2433.
- [5] Siavash A Bigdeli, Geng Lin, Tiziano Portenier, L Andrea Dunbar, and Matthias Zwicker. 2020. Learning generative models using denoising density estimators. *arXiv preprint arXiv:2001.02728* (2020).
- [6] Remi Cadene, Corentin Dancette, Matthieu Cord, Devi Parikh, et al. 2019. RUBi: Reducing unimodal biases for visual question answering. In *NeurIPS*. 841–852.
- [7] Long Chen, Xin Yan, Jun Xiao, Hanwang Zhang, Shiliang Pu, and Yueting Zhuang. 2020. Counterfactual samples synthesizing for robust visual question answering.

- In *CVPR*. 10800–10809.
- [8] Wenhui Chen, Zhe Gan, Linjie Li, Yu Cheng, William Wang, and Jingjing Liu. 2021. Meta module network for compositional visual reasoning. In *WACV*. 655–664.
 - [9] Yen-Chun Chen, Linjie Li, Licheng Yu, Ahmed El Kholy, Faisal Ahmed, Zhe Gan, Yu Cheng, and Jingjing Liu. 2020. UNITER: Universal image-text representation learning. In *ECCV*. 104–120.
 - [10] Christopher Clark, Mark Yatskar, and Luke Zettlemoyer. 2019. Don’t Take the Easy Way Out: Ensemble Based Methods for Avoiding Known Dataset Biases. In *EMNLP*. 4067–4080.
 - [11] Christopher Clark, Mark Yatskar, and Luke Zettlemoyer. 2020. Learning to Model and Ignore Dataset Bias with Mixed Capacity Ensembles. In *EMNLP*. 3031–3045.
 - [12] Quanyu Dai, Qiang Li, Jian Tang, and Dan Wang. 2018. Adversarial network embedding. In *AAAI*. 2167–2174.
 - [13] Nicola De Cao and Thomas Kipf. 2018. MolGAN: An implicit generative model for small molecular graphs. *arXiv preprint arXiv:1805.11973* (2018).
 - [14] Jacob Devlin, Ming-Wei Chang, Kenton Lee, and Kristina Toutanova. 2018. BERT: Pre-training of deep bidirectional transformers for language understanding. *arXiv preprint arXiv:1810.04805* (2018).
 - [15] Zhe Gan, Yen-Chun Chen, Linjie Li, Chen Zhu, Yu Cheng, and Jingjing Liu. 2020. Large-Scale Adversarial Training for Vision-and-Language Representation Learning. In *NeurIPS*.
 - [16] Difei Gao, Ke Li, Ruiping Wang, Shiguang Shan, and Xilin Chen. 2020. Multi-Modal Graph Neural Network for Joint Reasoning on Vision and Scene Text. In *CVPR*. 12746–12756.
 - [17] Itai Gat, Idan Schwartz, Alexander Schwing, and Tamir Hazan. 2020. Removing Bias in Multi-modal Classifiers: Regularization by Maximizing Functional Entropies. In *NeurIPS*.
 - [18] Tejas Gokhale, Pratyay Banerjee, Chitta Baral, and Yezhou Yang. 2020. MUTANT: A Training Paradigm for Out-of-Distribution Generalization in Visual Question Answering. In *EMNLP*. 878–892.
 - [19] Ian J Goodfellow, Jean Pouget-Abadie, Mehdi Mirza, Bing Xu, David Warde-Farley, Sherjil Ozair, Aaron Courville, and Yoshua Bengio. 2014. Generative adversarial networks. *arXiv preprint arXiv:1406.2661* (2014).
 - [20] Yash Goyal, Tejas Khot, Douglas Summers-Stay, Dhruv Batra, and Devi Parikh. 2017. Making the v in vqa matter: Elevating the role of image understanding in visual question answering. In *CVPR*. 6904–6913.
 - [21] Gabriel Grand and Yonatan Belinkov. 2019. Adversarial regularization for visual question answering: Strengths, shortcomings, and side effects. *arXiv preprint arXiv:1906.08430* (2019).
 - [22] Aditya Grover, Aaron Zweig, and Stefano Ermon. 2019. Graphite: Iterative generative modeling of graphs. In *ICML*. 2434–2444.
 - [23] Longteng Guo, Jing Liu, Jinhui Tang, Jiangwei Li, Wei Luo, and Hanqing Lu. 2019. Aligning linguistic words and visual semantic units for image captioning. In *ACM MM*. 765–773.
 - [24] Yangyang Guo, Zhiyong Cheng, Liqiang Nie, Yibing Liu, Yinglong Wang, and Mohan Kankanhalli. 2019. Quantifying and alleviating the language prior problem in visual question answering. In *SIGIR*. 75–84.
 - [25] Yangyang Guo, Liqiang Nie, Zhiyong Cheng, and Qi Tian. 2020. Loss-rescaling VQA: Revisiting Language Prior Problem from a Class-imbalance View. *arXiv preprint arXiv:2010.16010* (2020).
 - [26] Dan Hendrycks, Xiaoyuan Liu, Eric Wallace, Adam Dziedzic, Rishabh Krishnan, and Dawn Song. 2020. Pretrained transformers improve out-of-distribution robustness. *arXiv preprint arXiv:2004.06100* (2020).
 - [27] Ronghang Hu, Anna Rohrbach, Trevor Darrell, and Kate Saenko. 2019. Language-conditioned graph networks for relational reasoning. In *ICCV*. 10294–10303.
 - [28] Deng Huang, Peihao Chen, Runhao Zeng, Qing Du, Mingkui Tan, and Chuang Gan. 2020. Location-Aware Graph Convolutional Networks for Video Question Answering. In *AAAI*. 11021–11028.
 - [29] Drew A Hudson and Christopher D Manning. 2019. GQA: A new dataset for real-world visual reasoning and compositional question answering. In *CVPR*. 6700–6709.
 - [30] Pin Jiang and Yahong Han. 2020. Reasoning with heterogeneous graph alignment for video question answering. In *AAAI*. 11109–11116.
 - [31] Chenchen Jing, Yuwei Wu, Mingtao Pei, Yao Hu, Yunde Jia, and Qi Wu. 2020. Visual-Semantic Graph Matching for Visual Grounding. In *ACM MM*. 4041–4050.
 - [32] Chenchen Jing, Yuwei Wu, Xiaoxun Zhang, Yunde Jia, and Qi Wu. 2020. Overcoming Language Priors in VQA via Decomposed Linguistic Representations. In *AAAI*. 11181–11188.
 - [33] Yash Kant, Dhruv Batra, Peter Anderson, Alexander Schwing, Devi Parikh, Jiasen Lu, and Harsh Agrawal. 2020. Spatially aware multimodal transformers for textvqa. In *ECCV*. 715–732.
 - [34] Wataru Kawai, Yusuke Mukuta, and Tatsuya Harada. 2019. Scalable Generative Models for Graphs with Graph Attention Mechanism. *arXiv preprint arXiv:1906.01861* (2019).
 - [35] Corentin Kervadec, Grigory Antipov, Moez Baccouche, and Christian Wolf. 2020. Roses Are Red, Violets Are Blue... but Should Vqa Expect Them To? *arXiv preprint arXiv:2006.05121* (2020).
 - [36] Jin-Hwa Kim, Jaehyun Jun, and Byoung-Tak Zhang. 2018. Bilinear attention networks. In *NeurIPS*. 1564–1574.
 - [37] Diederik P Kingma and Max Welling. 2013. Auto-encoding variational bayes. *arXiv preprint arXiv:1312.6114* (2013).
 - [38] Thomas N Kipf and Max Welling. 2016. Semi-supervised classification with graph convolutional networks. *arXiv preprint arXiv:1609.02907* (2016).
 - [39] Thomas N Kipf and Max Welling. 2016. Variational graph auto-encoders. *arXiv preprint arXiv:1611.07308* (2016).
 - [40] Ranjay Krishna, Yuke Zhu, Oliver Groth, Justin Johnson, Kenji Hata, Joshua Kravitz, Stephanie Chen, Yannis Kalantidis, Li-Jia Li, David A Shamma, et al. 2017. Visual Genome: Connecting language and vision using crowdsourced dense image annotations. *IJCV* 123, 1 (2017), 32–73.
 - [41] Gouthaman KV and Anurag Mittal. 2020. Reducing Language Biases in Visual Question Answering with Visually-Grounded Question Encoder. In *ECCV*.
 - [42] Brenden M Lake, Tomer D Ullman, Joshua B Tenenbaum, and Samuel J Gershman. 2017. Building machines that learn and think like people. *Behavioral and brain sciences* 40 (2017).
 - [43] Linjie Li, Zhe Gan, Yu Cheng, and Jingjing Liu. 2019. Relation-aware graph attention network for visual question answering. In *ICCV*. 10313–10322.
 - [44] Linjie Li, Zhe Gan, and Jingjing Liu. 2020. A Closer Look at the Robustness of Vision-and-Language Pre-trained Models. *arXiv preprint arXiv:2012.08673* (2020).
 - [45] Zengyi Li, Yubei Chen, and Friedrich T Sommer. 2019. Learning energy-based models in high-dimensional spaces with multi-scale denoising score matching. *arXiv preprint arXiv:1910.07762* (2019).
 - [46] Zujie Liang, Weitao Jiang, Haifeng Hu, and Jiaying Zhu. 2020. Learning to Contrast the Counterfactual Samples for Robust Visual Question Answering. In *EMNLP*. 3285–3292.
 - [47] Renjie Liao, Yujia Li, Yang Song, Shenlong Wang, Charlie Nash, William L Hamilton, David Duvenaud, Raquel Urtasun, and Richard S Zemel. 2019. Efficient graph generation with graph recurrent attention networks. In *NeurIPS*. 4257–4267.
 - [48] Yongfei Liu, Bo Wan, Xiaodan Zhu, and Xuming He. 2020. Learning cross-modal context graph for visual grounding. In *AAAI*. 11645–11652.
 - [49] Nelson Nautata, Kai-Hung Chang, Chin-Yi Cheng, Greg Mori, and Yasutaka Furukawa. 2020. House-GAN: Relational generative adversarial networks for graph-constrained house layout generation. In *ECCV*. 162–177.
 - [50] Yulei Niu, Kaihua Tang, Hanwang Zhang, Zhiwu Lu, Xian-Sheng Hua, and Ji-Rong Wen. 2020. Counterfactual VQA: A Cause-Effect Look at Language Bias. *arXiv preprint arXiv:2006.04315* (2020).
 - [51] Shirui Pan, Ruiqi Hu, Guodong Long, Jing Jiang, Lina Yao, and Chengqi Zhang. 2018. Adversarially regularized graph autoencoder for graph embedding. In *IJCAI*. 2609–2615.
 - [52] Yanyuan Qiao, Zheng Yu, and Jing Liu. 2020. Rankvqa: Answer Re-Ranking For Visual Question Answering. In *ICME*. 1–6.
 - [53] Ramprasaath R Selvaraju, Stefan Lee, Yilin Shen, Hongxia Jin, Shalini Ghosh, Larry Heck, Dhruv Batra, and Devi Parikh. 2019. Taking a hint: Leveraging explanations to make vision and language models more grounded. In *ICCV*. 2591–2600.
 - [54] Chence Shi, Minkai Xu, Zhaocheng Zhu, Weinan Zhang, Ming Zhang, and Jian Tang. 2020. GraphAF: a flow-based autoregressive model for molecular graph generation. *arXiv preprint arXiv:2001.09382* (2020).
 - [55] Kevin J Shih, Saurabh Singh, and Derek Hoiem. 2016. Where to look: Focus regions for visual question answering. In *CVPR*. 4613–4621.
 - [56] Martin Simonovsky and Nikos Komodakis. 2018. Graphvae: Towards generation of small graphs using variational autoencoders. In *ICANN*. 412–422.
 - [57] Hao Tan and Mohit Bansal. 2019. LXMERT: Learning cross-modality encoder representations from transformers. In *EMNLP*. 5099–5110.
 - [58] Damien Teney, Ehsan Abbasnejad, and A. V. D. Hengel. 2020. Learning What Makes a Difference from Counterfactual Examples and Gradient Supervision. In *ECCV*. 580–599.
 - [59] Damien Teney, Ehsan Abbasnejad, and Anton van den Hengel. 2020. Unshuffling data for improved generalization. *arXiv preprint arXiv:2002.11894* (2020).
 - [60] Damien Teney and Anton van den Hengel. 2019. Actively seeking and learning from live data. In *CVPR*. 1940–1949.
 - [61] Damien Teney, Kushal Kafle, Robik Shrestha, Ehsan Abbasnejad, Christopher Kanan, and Anton van den Hengel. 2020. On the Value of Out-of-Distribution Testing: An Example of Goodhart’s Law. *arXiv preprint arXiv:2005.09241* (2020).
 - [62] Damien Teney, Qi Wu, and Anton van den Hengel. 2017. Visual question answering: A tutorial. 34, 6 (2017), 63–75.
 - [63] Petar Veličković, Guillem Cucurull, Arantxa Casanova, Adriana Romero, Pietro Lio, and Yoshua Bengio. 2017. Graph attention networks. *arXiv preprint arXiv:1710.10903* (2017).
 - [64] Pascal Vincent, Hugo Larochelle, Yoshua Bengio, and Pierre-Antoine Manzagol. 2008. Extracting and composing robust features with denoising autoencoders. In *ICML*. 1096–1103.
 - [65] Hongwei Wang, Jia Wang, Jialin Wang, Miao Zhao, Weinan Zhang, Fuzheng Zhang, Xing Xie, and Minyi Guo. 2018. Graphgan: Graph representation learning with generative adversarial nets. In *AAAI*. 2508–2515.

- [66] Jialin Wu and Raymond Mooney. 2019. Self-critical reasoning for robust visual question answering. In *NeurIPS*. 8604–8614.
- [67] Keyulu Xu, Weihua Hu, Jure Leskovec, and Stefanie Jegelka. 2018. How powerful are graph neural networks? *arXiv preprint arXiv:1810.00826* (2018).
- [68] Chao Yang, Su Feng, Dongsheng Li, Huawei Shen, Guoqing Wang, and Bin Jiang. 2020. Learning content and context with language bias for Visual Question Answering. *arXiv preprint arXiv:2012.11134* (2020).
- [69] Sibe Yang, Guanbin Li, and Yizhou Yu. 2020. Graph-structured referring expression reasoning in the wild. In *CVPR*. 9952–9961.
- [70] Ting Yao, Yingwei Pan, Yehao Li, and Tao Mei. 2018. Exploring visual relationship for image captioning. In *ECCV*. 684–699.
- [71] Jiaxuan You, Rex Ying, Xiang Ren, William L Hamilton, and Jure Leskovec. 2018. Graphrnn: Generating realistic graphs with deep auto-regressive models. In *ICML*. 5694–5703.
- [72] Yuning You, Tianlong Chen, Yongduo Sui, Ting Chen, Zhangyang Wang, and Yang Shen. 2020. Graph contrastive learning with augmentations. *arXiv preprint arXiv:2010.13902* (2020).
- [73] Wenqiao Yu, Cheng Zheng, Wei Cheng, Charu C Aggarwal, Dongjin Song, Bo Zong, Haifeng Chen, and Wei Wang. 2018. Learning deep network representations with adversarially regularized autoencoders. In *KDD*. 2663–2671.
- [74] Zhou Yu, Jun Yu, Yuhao Cui, Dacheng Tao, and Qi Tian. 2019. Deep modular co-attention networks for visual question answering. In *CVPR*. 6281–6290.
- [75] Peng Zhang, Yash Goyal, Douglas Summers-Stay, Dhruv Batra, and Devi Parikh. 2016. Yin and yang: Balancing and answering binary visual questions. In *CVPR*. 5014–5022.
- [76] Wenqiao Zhang, Haochen Shi, Siliang Tang, Jun Xiao, Qiang Yu, and Yueting Zhuang. 2021. Consensus graph representation learning for better grounded image captioning. In *AAAI*.
- [77] Shuai Zheng, Zhenfeng Zhu, Xingxing Zhang, Zhizhe Liu, Jian Cheng, and Yao Zhao. 2020. Distribution-induced Bidirectional Generative Adversarial Network for Graph Representation Learning. In *CVPR*. 7224–7233.
- [78] Xi Zhu, Zhendong Mao, Chunxiao Liu, Peng Zhang, Bin Wang, and Yongdong Zhang. 2020. Overcoming Language Priors with Self-supervised Learning for Visual Question Answering. In *IJCAI*. 1083–1089.
- [79] Zihao Zhu, Jing Yu, Yujing Wang, Yajing Sun, Yue Hu, and Qi Wu. 2020. Mucko: Multi-Layer Cross-Modal Knowledge Reasoning for Fact-based Visual Question Answering. *arXiv preprint arXiv:2006.09073* (2020).

A APPENDIX

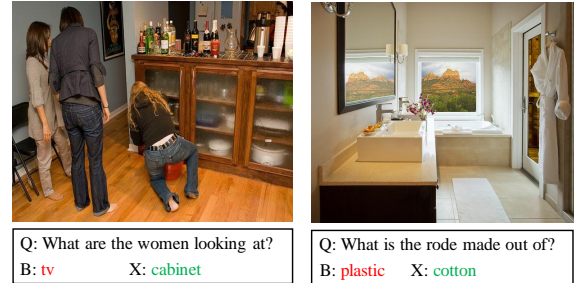
A.1 More Experimental Results

Ablation Studies. The results in Table 2 indicate that a single R-GGM or N-GGM can also effectively improve the OOD generalization ability of baseline VQA models in addition to the full X-GGM scheme, and \mathcal{L}_∇ is more effective than \mathcal{L}_D for alleviating the unstable gradient issue when training the baseline VQA model with the X-GGM scheme. To further illustrate the effectiveness of \mathcal{L}_∇ when training the Baseline with single R-GGM or N-GGM, as shown in Table 6 (#6, #7, #8, #9), we conduct more ablated experiments. Specifically, ▷ #6 only using \mathcal{L}_∇ as the adversarial loss to train the baseline VQA model (LXMERT) with the R-GGM. ▷ #7 only using \mathcal{L}_D as the adversarial loss to train the Baseline with the R-GGM. ▷ #8 only using \mathcal{L}_∇ as the adversarial loss to train the Baseline with the N-GGM. ▷ #9 only using \mathcal{L}_D as the adversarial loss to train the Baseline with the N-GGM. The results on VQA-CP v2 “Other” and GQA-OOD are shown in Table 6, which consistently illustrate that \mathcal{L}_∇ is more effective than \mathcal{L}_D when training the baseline VQA model with a single R-GGM or N-GGM.

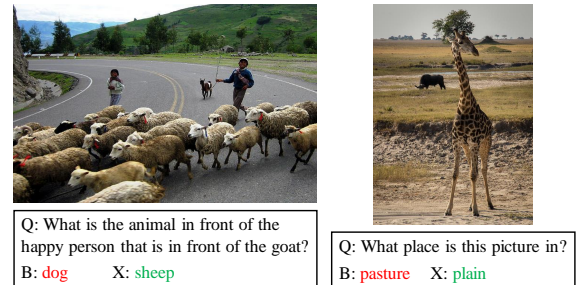
Comparisons with SoTAs on VQA-CP v2. Table 7 shows the full comparisons with state-of-the-art debiasing methods on VQA-CP v2. Compared with both KB-based and UB-based methods, the baseline VQA model (LXMERT) trained with the proposed X-GGM scheme can achieve state-of-the-art OOD and ID performance on VQA-CP v2 “Other”, further demonstrating the effectiveness of X-GGM to OOD generalization.

Table 6: Full ablation studies on R-GGM and N-GGM with different combinations of \mathcal{L}_∇ and \mathcal{L}_D .

S/N	R-GGM		N-GGM		VQA-CP v2			GQA-OOD		
	\mathcal{L}_∇	\mathcal{L}_D	\mathcal{L}_∇	\mathcal{L}_D	OOD↑	ID↑	Gap↓	Tail↑	Head↑	Δ ↓
LX.	—				59.98	65.21	5.23	49.80	57.70	15.90
#6	✓				63.37	65.71	2.34	51.36	56.95	10.88
#7		✓			62.67	65.21	2.54	50.80	57.13	12.45
#1	✓	✓			63.84	66.41	2.57	51.39	56.93	10.77
#8			✓		62.77	65.56	2.79	51.08	57.93	13.41
#9				✓	62.00	65.14	3.14	50.99	57.76	13.28
#2			✓	✓	62.90	65.57	2.67	51.27	57.30	11.76
#3	✓		✓		63.75	66.03	2.28	51.65	57.13	10.61
#4		✓		✓	62.73	65.99	3.26	51.27	57.19	11.54
#5	✓	✓	✓	✓	64.33	66.92	2.59	52.47	57.51	9.59



(a) VQA-CP v2 (OOD Test)



(b) GQA-OOD (Tail Test)

Figure 7: Qualitative examples respectively provided by the Baseline (B), i.e., LXMERT, and the Baseline trained with the X-GGM scheme (X). The wrong and correct answers are highlighted in red and green, respectively.

Additional Qualitative Examples. Like Figure 6, Figure 7 shows some additional qualitative examples from the OOD test set of VQA-CP v2 and GQA-OOD provided by the Baseline (i.e., LXMERT) and the Baseline trained with the X-GGM scheme.

Visualization of Relation Matrix. To further illustrate the process of graph generative modeling, considering the direct relation generation (i.e., R-GGM), Figure 8 compares the head maps of the pre-defined relation matrix R_{GT} and the generated relation matrix R_g of images which originate from the test set of GQA-OOD in Figure 6 and Figure 7. From the comparison between the heat maps of the pre-fined relation matrix and the generated one, we observe that correlations between nodes becomes more discriminative and new correlations are yielded after R-GGM.

Table 7: Comparisons with state-of-the-art debiasing methods on VQA-CP v2. †: methods using additional manually annotated data, *: results from our reimplementation using the official released code, -: not reported.

Method	VQA-CP v2 (OOD Test) ↑				VQA-CP v2 (ID Test) ↑				Gap ↓			
	All	Yes/No	Num.	Other	All	Yes/No	Num.	Other	All	Yes/No	Num.	Other
KB-based Methods												
RankVQA [52]	43.05	42.53	13.19	51.32	—	—	—	—	—	—	—	—
LM [10]	48.78	72.78	14.61	45.58	—	—	—	—	—	—	—	—
LMH [10]	52.01	72.58	31.12	46.97	—	—	—	—	—	—	—	—
+ LRS [25]	53.26	72.82	48.00	44.46	—	—	—	—	—	—	—	—
+ CCB+VQ-CSS [68]	59.12	89.12	51.04	45.62	—	—	—	—	—	—	—	—
+ MFE [17]	54.55	74.03	49.16	45.82	—	—	—	—	—	—	—	—
+ CSS+CL [46]	59.18	86.99	49.89	47.16	—	—	—	—	—	—	—	—
+ CSS+GS [46, 58]	57.37	79.71	50.85	47.45	—	—	—	—	—	—	—	—
+ CSS [7]	58.95	84.37	49.42	48.21	—	—	—	—	—	—	—	—
+ CCB [68]	57.99	86.41	45.63	48.76	—	—	—	—	—	—	—	—
+ MCE (LXMERT) [11]	70.32	—	—	—	70.78	—	—	—	0.46	—	—	—
UB-based Methods												
GVQA [2]	31.30	57.99	13.68	22.14	—	—	—	—	—	—	—	—
Actively Seeking [60]	46.00	58.24	29.49	44.33	—	—	—	—	—	—	—	—
Unshuffling+CF+GS [58]	46.80	64.50	15.30	45.90	62.40	77.80	43.80	53.60	15.60	13.30	28.50	7.70
Unshuffling+CF [58]	40.60	61.30	15.60	46.00	63.30	79.40	45.50	53.70	22.70	18.10	29.90	7.70
VGQE [41]	50.11	66.35	27.08	46.77	—	—	—	—	—	—	—	—
Unshuffling [59]	42.39	47.72	14.43	47.24	—	—	—	—	—	—	—	—
UpDn [3]	38.82	42.98	12.18	43.95	64.73	79.45	49.59	55.66	25.91	36.47	37.41	11.71
+ Top answer masked [61]	40.61	82.44	27.63	22.26	30.90	44.12	5.00	20.85	9.71	38.32	22.63	1.41
+ AdvReg [21]	36.33	59.33	14.01	30.41	50.63	67.39	38.81	38.37	14.30	8.06	24.80	7.96
+ GRL [21]	42.33	59.74	14.78	40.76	56.90	69.23	42.50	49.36	14.57	9.49	27.72	8.60
+ RUBi [6]	47.11	68.65	20.28	43.18	—	—	—	—	—	—	—	—
+ RandImg ($\lambda=12$) [61]	55.37	83.89	41.60	44.20	54.24	64.22	34.40	50.46	1.13	19.67	7.20	6.26
+ CF-VQA (Sum) [50]	53.69	91.25	12.80	45.23	—	—	—	—	—	—	—	—
+ CF-VQA (Har.) [50]	49.94	74.82	18.93	45.42	—	—	—	—	—	—	—	—
+ DLR [32]	48.87	70.99	18.72	45.57	—	—	—	—	—	—	—	—
+ RandImg ($\lambda=5$) [61]	51.15	75.06	24.30	45.99	59.28	70.66	43.06	53.40	8.13	4.40	18.76	7.41
+ HINT(HAT) [†] [53]	47.70	70.04	10.68	46.31	—	—	—	—	—	—	—	—
+ SCR (HAT) [†] [66]	49.17	71.55	10.72	47.49	—	—	—	—	—	—	—	—
+ SCR (VQA-X) [†] [66]	49.45	72.36	10.93	48.02	—	—	—	—	—	—	—	—
+ SL [78]	57.59	86.53	29.87	50.03	—	—	—	—	—	—	—	—
+ MUTANT [†] [18]	61.72	88.90	49.68	50.78	—	—	—	—	—	—	—	—
+ X-GGM	45.71	43.48	27.65	52.34	67.16	83.74	48.26	56.91	21.45	40.26	20.61	4.57
MANGO [44]	52.76	—	—	—	—	—	—	—	—	—	—	—
LXMERT* [57]	63.90	80.45	46.58	59.98	75.57	91.39	59.83	65.21	11.67	10.94	13.25	5.23
+ MUTANT [†] [18]	69.52	93.15	67.17	57.78	—	—	—	—	—	—	—	—
+ VILLA* [15]	48.06	42.66	18.97	58.89	75.85	90.40	60.02	66.66	27.79	47.97	41.05	7.77
+ MCE+Adv [11]	66.08	—	—	—	77.17	—	—	—	11.09	—	—	—
+ MCE [11]	68.44	—	—	—	74.03	—	—	—	5.59	—	—	—
+ X-GGM	66.95	78.91	53.63	64.33	75.88	90.18	60.06	66.92	8.93	11.27	6.43	2.59

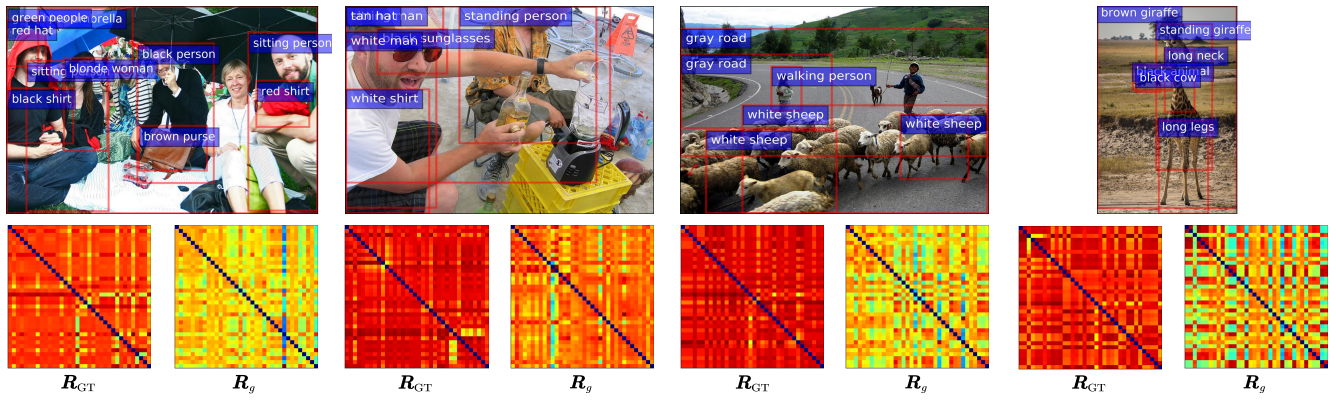


Figure 8: Heat maps of relation matrices. R_{GT} is the pre-defined relation matrix (*i.e.*, the cosine similarity between object-class embeddings and object-attribute embeddings on the image), R_g is the generated relation matrix during R-GGM.